



Dry Sliding Behavior of Carbon-based Brake Pad Materials

U. V. Saindane*, S. Soni, J. V. Menghani

Mechanical Engineering Department, Sardar Vallabhbhai National Institute of Technology, Surat, India

PAPER INFO

Paper history:

Received 11 September 2021

Received in revised form 28 September 2021

Accepted 05 October 2021

Keywords:

Brake Materials

Dry Sliding

Friction Coefficient

Friction Materials

Pin on Disc

Wear

ABSTRACT

The brake pad plays a crucial role in the control of vehicle and machinery equipment and subsequent safety. There is always a need for a new functional material with improved properties than existing ones. The present research study was carried out to develop a new brake pad material made up of polymer nanocomposite for enhanced physical, mechanical, and frictional characteristics in comparison to existing brake pad materials. In this study, polymer nanocomposite samples were developed and their physical properties namely density, water-oil absorption, and porosity were evaluated. Mechanical hardness of developed samples was estimated with Vicker's hardness tester. Frictional characteristics of samples and wear values determined with pin or disc apparatus. Dry sliding behavior was examined by conducting multiple trials with sliding speed in the span of 2-10 m/s and load were changed from 20 N to 100 N to discuss the effect of velocity, the effect of nominal contact pressure and the effect of sliding distance on friction and temperature parameters. Morphology of prepared brake pad samples was characterized with the scanning electron microscope. Scanning electron micrographs of brake pad surfaces showed different shape wear debris and plateaus significantly affecting the friction characteristics. Developed samples along with commercial specimens show excellent resistance to water and oil absorption. Thus obtained results for evaluated polymer nanocomposite brake pad samples demonstrate their potential for brake pad applications.

doi: 10.5829/ije.2021.34.11b.14

NOMENCLATURE

FBP	Fabricated brake pad	POD	Pin on Disc
CBP	commercial brake pad	SCF	short carbon fibers
COF	Coefficient of friction	CNT	carbon nanotubes
MWCNT	Multiwall carbon nanotubes	WA	Water absorption
CI	Cast iron	OA	Oil absorption

1. INTRODUCTION

The braking mechanism is a critical part of cars and machinery equipment. As opposed to drum brakes, most cars now use disc brakes because they escape heat faster and thus reduce fade. Brake pads transform the vehicle's kinetic energy to thermal energy. The brake pad is making contact with the disk to provide force for stopping, it gets heated up as a result minor quantities of friction compounds are transferred to the disc or pad [1]. However, no particular material could meet the expected performance-related requirements like safety and

reliability under different brake conditions in a disc brake system. The friction materials must provide a stable COF and high wear resistance at different operating pressures, speeds, environmental conditions and temperatures. Additionally, these materials should be compliant with the material of the rotor to minimize wear of rotor, friction, and braking noise [2].

Some of the unique benefits of hybrid composites over traditional composites are balanced strength and stiffness, balanced bending and membrane mechanical characteristics, balanced thermal distortion stability, and decreased cost and weight. Various hybrid composite

*Corresponding Author Institutional Email:
ds17me002@med.svnit.ac.in (U. V. Saindane)

materials have been investigated and used as brake pads for automobiles in recent years [3]. Brake pads consist of more than 10 different ingredients, reinforcing fibers, resin as a binder, solid lubricants, abrasives, wear-resistant and friction modifiers are often used in these components. The type and quantity of these constituents are often decided by practice, empirical observation or a trial-and-error approach for developing a new combination. Asbestos has been a common ingredient in brake pads for the past twenty years because of its resilience, heat resistance, and fire resistance. Since asbestos emits toxic substances that can cause lung cancer and affect health adversely, it has been banned from being used as a component in the manufacture of brake pads since 1980s. Therefore, asbestos was replaced with non-asbestos materials such as Kevlar (aramid fiber), glass fiber, and graphite [4, 5]. However alternatives such as Kevlar, glass fiber and graphite did not compete with the friction performance of materials containing carbon fibers [6]. Carbon fibers provide a stable coefficient of friction (0.4-0.5) throughout the braking operation [7]. An attempt has been made in this paper to manufacture the composite samples with short carbon fibers as the main reinforcement.

Considering the advantage of carbon fibers as brake pad additive material, recently [8] has developed short carbon fiber reinforced epoxy composites. The use of SCF additive in epoxy composite significantly reduced the immediate contact between the counterpart and composite. While the use of CNT and graphene powder in brake pad epoxy composite, also improved the mechanical characteristics and thermal conductivity of the composite [9].

In consistency with the latest efforts for the development of new and effective brake pad materials, [10] have designed and developed two polymer nanocomposites made up of epoxy polymer, multiwalled carbon nanotubes, graphene and carbon fibers.

The present study compares a possibly modern fabricated non-asbestos carbon-based brake pad (FBP) to a non-asbestos commercial brake pad (CBP) to test and examine their tribological properties. Both FBP and CBP were tested by measuring hardness, density, water and oil absorption. Pin on Disc type tribometer test machine was used to carry out tribological tests. Grey cast iron rotor disc was used to test the friction materials. The test was conducted under the effect of load (20-100 N), sliding speed (2-10 m/s) and sliding distance up to (2.7 km).

2. EXPERIMENTAL PROCEDURE

Jai Rubber Enterprises, Pune has supplied the woven carbon fabric and epoxy resin of grade 650 and hardener form from Adnano technologies pvt. ltd., Shimoga,

Karnataka. Molybdenum disulfide powder was obtained from Premier industrial corporation Ltd., Mumbai.

2. 1. Preparation of Pad Specimens

FBP samples were manufactured using the hand lay method in this work. The detailed procedure was explained in the work [10]. The ingredients and their proportion were represented in Table 1. The fabricated sample was made by mixing powdered and epoxy resin materials. Epoxy resin, multi-wall carbon nanotubes and graphite nanopowder were manually mixed for 20 minutes to achieve a homogenous solution. Tiny, 5-10 mm long carbon fibers are then mixed with a combination of epoxy and nanocomposites. This blend is then mixed manually for a further ten minutes. The plastic mold measuring 50 mm x 50 mm x 15 mm was used to prepare the fabricated brake pad. Wax was added to the mold's inner surface before pouring to make the composite easy to remove. The mixture was subsequently poured into a 12 mm deep open mold. The mix was permitted to cure for two days at room temperature in the mold. After two days of proper curing, the composite mixture was removed. Sample was polished to a smooth surface finish. Figure 1 depicts a polished sample. Commercial brake pad sample was chosen from brake pad samples available in the market. The fabricated brake pad sample was compared with chosen commercial brake pad sample. The chosen brake pad sample was used in the Bajaj Pulsar two-wheeler automobile shown in Figure 2.

2. 2. Hardness and Density Test

Vickers hardness tester was used to conduct the hardness test. Because the Vickers technique covers the full hardness



Figure 1. Fabricated brake pad sample (FBP)



Figure 2. Commercial brake pad sample (CBP)

TABLE 1. Physical properties of ingredients

Sr. No.	Ingredient	Density (g/cm ³)	Viscosity (mPas)	Size	Colour
1	Epoxy Resin (650)	1.13	800-1000	-	Semi transparent
2	Hardner (651)	1.019	650	-	Yellow
3	Short carbon fibers	2	-	L=5-10 mm	
4	MWCNT	0.14	-	L=1-20 μm, D=10-30 nm	Black
5	Graphene	1-2.39	-	D=<10 0 nm	Iron black
6	Molybdenum disulfide	5.06	-	D=10-30 μm	Grey

range, it could be used on all materials and test specimens, from soft to hard [11]. Each sample was indented three times with a diamond indenter, and the average of the diagonals in all three indentations was used to calculate the results, as shown in Figure 5. Equation (1) was used for hardness calculation.

$$HV = 1.854 \times \left(\frac{F}{d^2} \right) \quad (1)$$

$$\text{Where, } F = \text{Load in kgf, } d = \left(\frac{d_1 + d_2}{2} \right)$$

The Archimedeon technique was used to determine the density of the composites. The difference in water level between samples was measured after they have been fully immersed in water. According to the concept, 1 ml of water displaced equals 1 cm³ of body volume submerged in that water. Finally, the density of samples was determined by the mass to volume ratio [12].

2. 3. Water and Oil Absorption Test The test was done in accordance with the ASTM D 570-98 test specification [13]. To disperse heat generated during braking, porosity is necessary. The samples were thoroughly immersed in the engine oil of grade 10W-30 from the Mak 4t Zipp brand of Bharat Petroleum Corporation Ltd. for the oil absorption test. The initial and end weights of the samples were determined, and the percent oil absorption was computed using Equation (2).

$$\% \text{Oil Absorption} = \left(\frac{\text{Final weight} - \text{Initial weight}}{\text{Initial weight}} \times 100 \right) \quad (2)$$

2. 4. Porosity Test Standard JIS D 4418-1996 was used to measure porosity [14]. The specimens were sliced to 15 × 15 × 5 mm³ each and weighed (M₁). The sliced samples were then placed in a desiccator for 24 hours at ambient temperature. The samples were then

kept in an oil container and heated to 85°C for 7 hours. The samples were then put into the oil tank for the next 12 hours to achieve room temperature. After removing the samples from the oil tank, the oil had been removed using a cloth. Finally the samples were weighed (M₂). The density (ρ) and volume (V) of the samples were also determined. The porosity (P) in percent was calculated using the following Equation (3).

$$P(\%) = \left(\frac{M_2 - M_1}{\rho} \right) \times \left(\frac{1}{V} \right) \times 100 \quad (3)$$

2. 5. Counter Disc Material To assess the wear, grey cast iron of grade 4 E was utilized. The disc has a hardness rating of 190 HV. The disc had an average surface roughness of 2.2 ± 0.2 μm.

2. 6. Test Set up and Procedures POD type apparatus was utilized to perform tribo test as seen in Figure 3 to study the work in progress at and medium nominal contact pressure (upto1 Mpa) and high speed (up to 10 m/s). Specimen of fabricated brake pad sample was prepared in the form of the pin shown in Figure 4. Dry sliding tests were carried out at room temperature and ambient humidity, with sliding speed in the span of 2-10 m/s and the load were changed from 20 N to 100 N. 10 dry tests were performed on 10 different specimens prepared of fabricated brake pad for various speeds (2 - 10 m/s) and various load conditions (20 -100 N). The next 10 run of dry tests were performed on 10 distinct specimens prepared of commercial brake pad sample under the same velocity and load conditions [15]. To ensure that the two rubbing surfaces make excellent, consistent contact, rubbing of pad specimens was carried out with a silicon abrasive paper before the tests. i. e. contacting surfaces. The frictional force was measured using a strain guage present at the level arm that holds the specimen. The coefficient of friction value was calculated using the ratio of frictional force to normal load. Wear was determined in the form of weight loss

**Figure 3.** Pin on Disc tribo tester



Figure 4. Specimen Pins

during the test [16]. The microstructures of worn-out surfaces were determined using scanning electron microscope Hitachi S- 3400 N.

2. 7. Temperature Measurement STANLEY STHT0-77365 high accuracy industrial digital infrared thermometer was used to know the temperature during surface interaction. The infrared thermometer was kept approximately 12 cm away from the trailing edge of the brake pad specimen.

3. RESULTS AND DISCUSSION

The values of characterization for both brake materials are tabulated. The measured values of physical and mechanical characteristics of both the samples are lies in the range of acceptable limits (Table 2).

3. 1. Physical and Mechanical Properties An Increase in hardness of FBP was found significant compare to the CBP sample. The strength of short carbon fibers and multi-wall carbon nanotubes increased the hardness. The presence of carbon fiber content in the composite decreased the FBP sample's density [12]. This may be due to void formation due to carbon fibers, as a result porosity has increased (2.1%) [17]. The absorption of the heat generated mainly depends on porosity. High porosity leads to enhanced friction coefficient and high wear rate as contact area increases for FBP than CBP in the current study. Water and Oil absorption values were representing the moisture content for FBP and CBP. High values of water and oil absorption were observed for FBP as compared to CBP due to the carbon-based ingredients

used in FBP, which may deteriorate the fiber-matrix interface and change the sample dimensions.

3. 2. Wear Test The surface films developed due to friction between the disc and pad interface. Some authors claimed that this can lead to a steady friction pattern, but their precise function in braking is still tendentious [18]. Addition of abrasive additives in friction materials is used to control the growth of friction film developed on the rotor disc surface and to improve the grip between pad and disc [19]. The mechanism of steady friction using the third body system remain to be expressive. The driver's key worry was the brake pad's effective functioning under various braking conditions. It was therefore necessary to present changes in COF as a function of the speed of sliding and load applied or contact pressure.

3. 3. Effect of Sliding Speed Figure 5 shows the effect of the speed of sliding on friction and wear properties under a continuous load of 45 N, corresponding to 0.4 MPa nominal contact pressure, over a test duration of 300 seconds. The impact of speed of sliding on friction, thermal and wear rate performance was seen in Figure 5, when tested at a constant normal load 45 N i.e. contact pressure (nominal) of 0.4 MPa for 300 seconds. The friction coefficient shows a 'increasing-steady state decreasing' pattern in Figure 5 (a) for both friction materials namely fabricated brake pad and commercial brake pad. The generation of cold welding and breakup of asperities on the fresh friction surface must have caused the rising trend in COF i.e. from 0.31 to 0.38 for CBP and 0,36 to 0.44 for FBP at the start of the dry sliding test.

As a result, the temperature of the interfaces increased throughout the test, which later was verified by a visual inspection of Figure 5 (b). Illustrating that as the sliding speed increases, the temperature rises linearly ie from 48 °C to 68 °C for CBP and from 60 °C to 89 °C for FBP. A similar trend was reported by Österle et al. [20]. It was discovered that the test specimen's uneven surface can lead to the formation of a separate body between the pad and disc surfaces. These third entities can help with film transfer onto the sliding counterface by moving between the interfaces in a circular or linear motion [21]. During the adhesive dry test, this raised the friction coefficient, resulting in a considerably higher contact temperature. When the contact temperature reached 6 m/s, the COF of all brake pad samples started to fall as a result of loss of

TABLE 2. Physical and mechanical properties

	Hardness (HV 70)	Density (gm/cc)	WA (%)	OA (%)	Porosity (W) %	Porosity (O) %
FBP	195	0.8591	0.0277	0.0094	2.1	0.113
CBP	177	1.8667	0.0324	0.01022	1.16	0.086

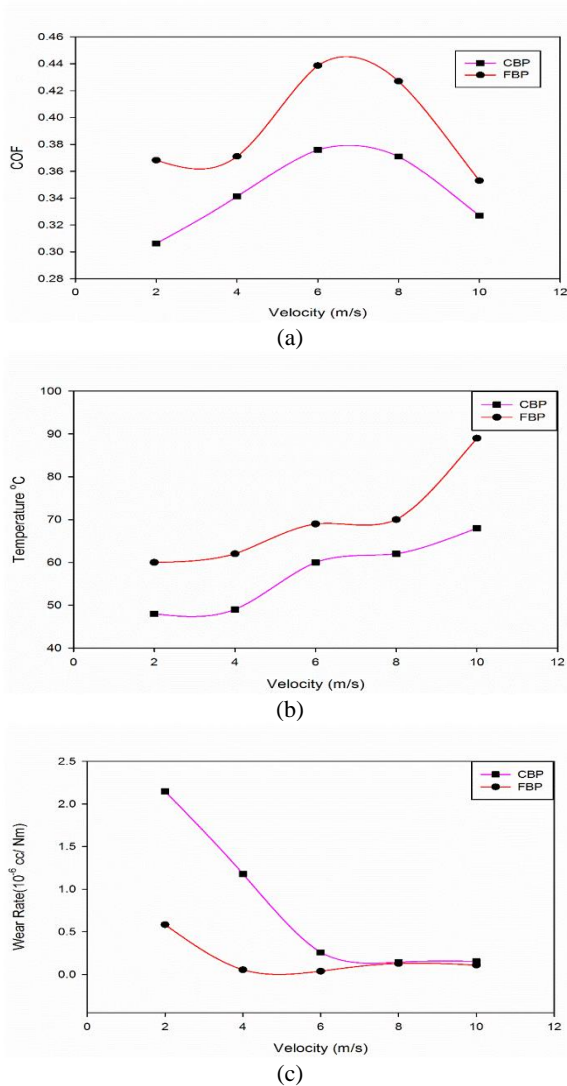


Figure 5. Changes in (a) friction, (b) interface temperature, and (c) wear for FBP and CBP materials exposed to a constant nominal load of 45 N for a test duration of 300 seconds

friction owing to frictional heating, When the contact temperature reached 8 m/s, the COF of all brake pad materials started to fall as a result of frictional heating, called as fade.

Alternatively, for both brake pad compositions, there was evidence of a 'running in' phase of wear rate, as shown in Figure 5(c). When the wear rate was raised to 6 m/s, the variations in wear characteristics between the two friction materials were no longer as evident as they had been in the 'running in' area i.e. reduced from 0.018 to 0.012 gm. When the speed of sliding was more than 6 m/s, the COF also began to decline till further decline up to the value 0.327 which was seen in Figure 5(a). This might be owing to the fast layer transfer to the

counterface, which resulted in the development of a thin shield film that prevents the brake pad material's wear rate from increasing any further [22].

3. 3. Effect of Normal Load

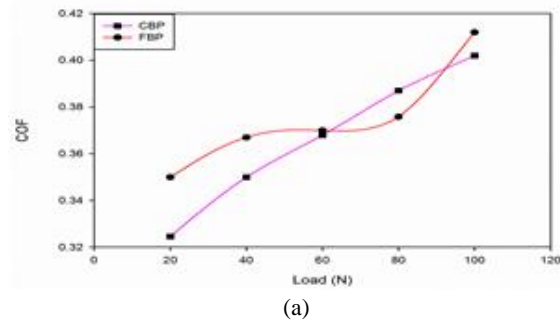
The impact of normal load on friction and wear characteristics for two distinct friction materials subjected to constant velocity 4 m/s for the duration of test 300 s is presented in Figure 6.

Friction and temperature profiles of both brake pads show a general upward tendency with increasing normal load, Figures 6(a) and 6(b). This leads to a considerable temperature increase as well as an increase in COF i.e. from 60 °C to 84 °C and from 0.33 to 0.40 for temperature and COF respectively. The current study's findings are consistent with finding reported by Österleet al. [20] who showed that in a wide variety of operating conditions, a reliable brake pad material must retain good stability of friction except at load 100 N decrease in temperature from 84°C to 79°C was attributed to uncertainties and errors during experiments [23].

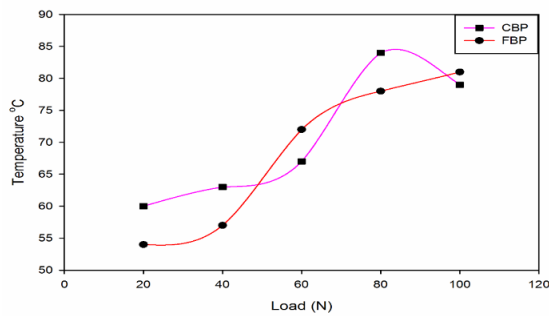
The wear rate of both friction materials, on the contrary, showed a non-linear gradual decline as contact pressure increased, as shown in Figure 6(c). Wear rate decline from 0.84 10⁻⁶ ml/Nm to 0.11 10⁻⁶ ml /Nm for CBP and from 2.57 10⁻⁶ ml /Nm to 0.20 10⁻⁶ ml /Nm for FBP. Thus in comparison to the CBP, the FBP had the superior overall wear performance. The carbon fiber content in test specimens would account for FBP's excellent wear resistance [24]. The chances of a third-body contact across the sliding surfaces were reduced as a result, thus decreases abrasive wear that may have led to a high rate of material loss during the test.

3. 4. Effect of Sliding Distance

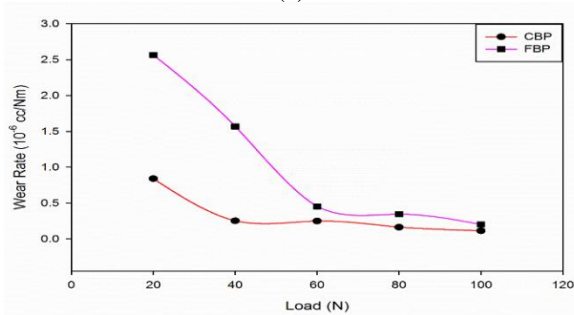
When two brake pad materials are subjected to a constant speed of sliding 10 m/s and fixed nominal contact pressure of 0.4 MPa, The friction and temperature response concerning sliding distance is shown in Figure 7. The adherence of brake pad metal chips to the friction surface of the cast-iron disc is typically linked to a continual rise in the friction coefficient [25]. Both friction materials exhibit stability of coefficient of friction after 7 km, as shown in Figure



(a)

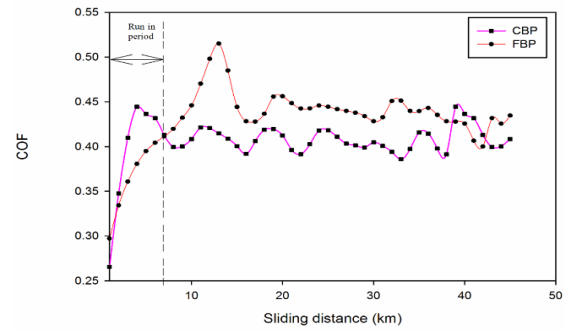


(b)

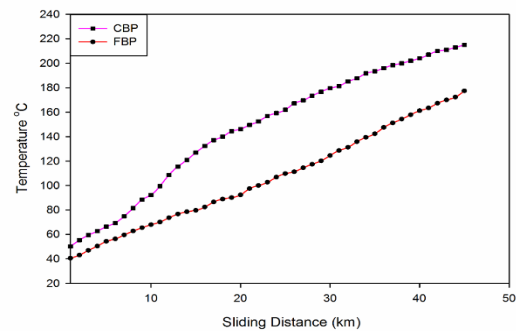


(c)

Figure 6. Variations in (a) coefficient of friction, (b) interface temperature, and (c) wear for FBP and CBP materials exposed to a constant sliding speed of 4 m/s for 300 seconds.



(a)



(b)

Figure 7. Changes in (a) coefficient of friction and (b) temperature for CBP and FBP materials at varied sliding distances under dry sliding conditions: 10 m/s and 0.4 MPa

7(a).The range of COF lies in 0.26 to 0.44 for CBP and lies in 0.39 to 0.51 for FBP respectively. This is due to a homogeneous transfer of the film on the surface of rotor disc, which explains the determined value of steady friction performance at higher temperatures, as shown in Figure 7. When the sliding distance was increased, all of the test specimens saw a consistent rise in temperature, as seen in Figure 7(b) maximum rise in temperature for CBP was observed to 215 °C and for FBP temperature rise was up to 177.4 °C. This is due to the specimens slide against the grey CI disc continually, a process known as adhesive dry sliding.

3. 5. SEM Analysis

The different reinforcing stages were identified and found to be equally distributed, demonstrating the fabricated brake pad's homogeneity. Figure 8 depicts the microstructure of FBP, which shows tiny cracks that have little effect on the coefficient of friction or wear. Wear debris in the shape of plates was discovered, indicating good wear resistance.

The micrographs of the worn surface of CBP showed more pulled-out fiber, greater debonding of the fiber matrix, and substantial degradation in filler matrix bonding as shown in Figure 9. Roughness and specific wear rate are increased as a result of the pulled-out fibers [26]. Low wear resistance is indicated by fine spherical wear debris.

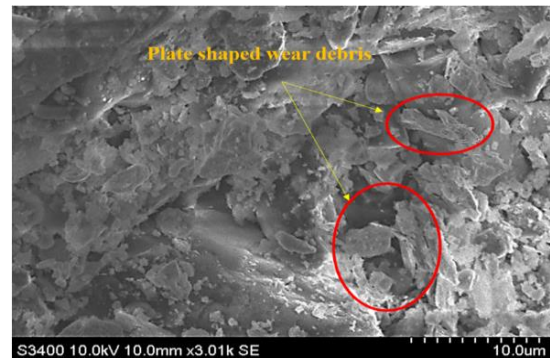


Figure 8. Microstructure of FBP

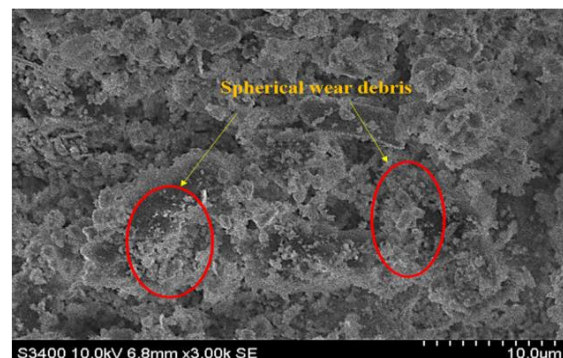


Figure 9. Microstructure of CBP

4. CONCLUSIONS

In a dry sliding test, the impact of speed of sliding, nominal contact pressure, and distance of sliding on friction coefficient (COF), wear rate, and temperature for FBP and CBP were investigated. The findings of this research and evaluation are listed below.

1. The influence of sliding speed on COF revealed an 'increasing-steady state decreasing' pattern for all materials. In comparison to CBP, FAB has the greatest COF (0.439). The lower COF went to CBP (0.341). As the temperature rose, frictional heating caused the COF of all materials to decrease. When the speed of sliding was more than 6 m/s, however, the wear rate for all materials decreased. this may be due to the creation of a transfer layer that shields the brake pad from fast wear.
2. The results revealed that FAB had the highest COF under normal load, and that it increased with the load.
3. Meanwhile, FBP had the fewest fluctuations and CBP had shown lower COF (0.35). In other words, FAB worked well under the influence of varying normal load since friction materials are anticipated to maintain a consistent COF (0.41) over a wide range of braking situations. When the normal load rose, the wear performance of both friction materials followed the sequence CBP > FBP, with FBP exhibiting strong wear resistance and a steady COF.
4. FAB was also successful in stabilizing the friction coefficient. for a large sliding distance (42 km).
5. At higher contact temperatures, Frictional performance is significantly influenced by the layer formed on the friction surface, which enhances the stability of the friction coefficient, as a result, improves fade resistance.
6. Physical and mechanical properties exhibited by FAB are much better than CBP. As a result, it is directly equivalent to CBP material, which contains asbestos and has excellent frictional properties.

5. REFERENCES

1. M. Akhondizadeh, M. Fooladi Mahani, S. H. Mansouri, M. Rezaeizadeh, "A New Procedure of Impact Wear evaluation of Mill Liner", *International Journal of Engineering, Transactions A: Basics.*, Vol. 28, No. 4, (2015), 593-598.
2. D. Mehra, M. M. Mahapatra, and S. P. Harsha, "Effect of wear parameters on dry abrasive wear of RZ5-TiC in situ composite," *Industrial Lubrication and Tribology*, Vol. 70, No. 2, (2018), 256-263, doi: 10.1108/ILT-12-2016-0306.
3. T. R. Jaafar, N. I. Ismail, M. F. Ismail, and E. A. Othman, "Influence of steel fibres on friction behaviours with respect to speed, pressure and temperature" *Industrial Lubrication and Tribology*, Vol. 69, No. 3, (2017), 420-424, doi: 10.1108/ILT-09-2016-0230.
4. N. Aranganathan, V. Mahale, and J. Bijwe, "Effects of aramid fiber concentration on the friction and wear characteristics of non-asbestos organic friction composites using standardized braking tests," *Wear*, Vol. 354-355, (2016), 69-77, doi: 10.1016/j.wear.2016.03.002.
5. T. Singh and A. Patnaik, "Performance assessment of lapinus-aramid based brake pad hybrid phenolic composites in friction braking," *Archives of Civil and Mechanical Engineering.*, Vol. 15, No. 1, (2015), 151-161, doi: 10.1016/j.acme.2014.01.009.
6. C. Capela, S. E. Oliveira, and J. A. M. Ferreira, "Mechanical behavior of high dosage short carbon fiber reinforced epoxy composites," *Fibers and Polymers*, Vol. 18, No. 6, (2017), 1200-1207, doi: 10.1007/s12221-017-7246-0.
7. F. Ahmadijokani, Y. Alaei, A. Shojaei, M. Arjmand, and N. Yan, "Frictional behavior of resin-based brake composites: Effect of carbon fibre reinforcement," *Wear*, Vol. 420-421, (2019), 108-115, doi: 10.1016/j.wear.2018.12.098.
8. N. W. Khun, H. Zhang, L. H. Lim, C. Y. Yue, X. Hu, and J. Yang, "Tribological properties of short carbon fibers reinforced epoxy composites," *Friction*, Vol. 2, No. 3, (2014), 226-239, doi: 10.1007/s40544-014-0043-5.
9. S. Y. Yang Yang, S.Y., Lin, W.N., Huang, Y.L., Tien, H.W., Wang, J.Y., Ma, C.C.M., Li, S.M. and Wang, Y.S., "Synergetic effects of graphene platelets and carbon nanotubes on the mechanical and thermal properties of epoxy composites," *Carbon*, Vol. 49, No. 3, (2011), 793-803, doi: 10.1016/j.carbon.2010.10.014.
10. U. V. Saindane, S. Soni, and J. V. Menghani, "Studies on mechanical properties of brake friction materials derived from carbon fibres reinforced polymer composite," *Materials. Today Proceedings.*, (2021), doi: 10.1016/j.matpr.2021.04.079.
11. P. Thiyagarajan, "Controlling the Hardness and Tribological Behaviour of Non-asbestos Brake Lining Materials for Automobiles," *Carbon Letters*, Vol. 5, No. 1, (2004), 6-11,
12. M. Ünalı and R. Kuş, "The Determination of the Effect of Mixture Proportions and Production Parameters on Density and Porosity Features of Miscanthus Reinforced Brake Pads by Taguchi Method," *International Journal of Automotive Engineering and Technologies*, Vol. 7, No. 1, (2018), 48-57, doi: 10.18245/ijaet.438047.
13. S. D. 50 on permanence properties ASTM committee on D-20 on plastics, "Standard test Method for Water Absorption of Plastics," American Society for Testing and Materials. (1995).
14. Japan Industrial standard, "Test procedures of Porosity for Brake Linings and Pad Formulations. JIS D 4418." (1996).
15. K. W. Liew and U. Nirmal, "Frictional performance evaluation of newly designed brake pad materials," *Materials and Design*, Vol. 48, (2013), 25-33, doi: 10.1016/j.matdes.2012.07.055.
16. C. Menapace, M. Leonardi, V. Matějka, S. Gialanella, and G. Straffelini, "Dry sliding behavior and friction layer formation in copper-free barite containing friction materials," *Wear*, Vol. 398-399, (2018), 191-200, doi: 10.1016/j.wear.2017.12.008.
17. Sellami, M. Kchaou, R. Elleuch, A. L. Cristol, and Y. Desplanques, "Study of the interaction between microstructure, mechanical and tribo-performance of a commercial brake lining material," *Materials and Design*, Vol. 59, (2014), 84-93, doi: 10.1016/j.matdes.2014.02.025.
18. A. Shojaei, M. Arjmand, and A. Saffar, "Studies on the friction and wear characteristics of rubber-based friction materials containing carbon and cellulose fibers," *Journal of Materials Science*, Vol. 46, No. 6, (2011), 1890-1901, doi: 10.1007/s10853-010-5022-2.
19. L. Wei, Y. S. Choy, C. S. Cheung, and D. Jin, "Tribology performance, airborne particle emissions and brake squeal noise of copper-free friction materials," *Wear*, (2020), 448-449. doi: 10.1016/j.wear.2020.203215.
20. W. Österle, Dörfel, I., Prietzel, C., Rooch, H., Cristol-Bulthé, A.L., Degallaix, G. and Desplanques, Y., "A comprehensive

- microscopic study of third body formation at the interface between a brake pad and brake disc during the final stage of a pin-on-disc test," *Wear*, Vol. 267, No. 5-8, (2009), 781-788, doi: 10.1016/j.wear.2008.11.023.
21. N. S. M. EL-Tayeb and K. W. Liew, "On the dry and wet sliding performance of potentially new frictional brake pad materials for automotive industry," *Wear*, Vol. 266, No. 1-2, (2009), 275-287, doi: 10.1016/j.wear.2008.07.003.
 22. N. Elzayady and R. Elsoeudy, "Microstructure and wear mechanisms investigation on the brake pad," *Journal of Materials Research and Technology*, Vol. 11, (2021), 2314-2335, doi: 10.1016/j.jmrt.2021.02.045.
 23. R. J. Moffat, "Describing the uncertainties in experimental results," *Experimental Thermal and Fluid Science*, Vol. 1, No. 1, (1988), 3-17, doi: 10.1016/0894-1777(88)90043-X.
 24. O. J. Gbadeyan, K. Kanny, and T. P. Mohan, "Influence of the multi-walled carbon nanotube and short carbon fibre composition on tribological properties of epoxy composites," *Tribology-Materials, Surfaces & Interfaces*, Vol. 11, No. 2, (2017), 59-65, doi: 10.1080/17515831.2017.1293763.
 25. K. W. Hee and P. Filip, "Performance of ceramic enhanced phenolic matrix brake lining materials for automotive brake linings," *Wear*, Vol. 259, No. 7-12, (2005), 1088-1096, doi: 10.1016/j.wear.2005.02.083.
 26. ÖZtürk, F. Arslan, and S. Öztürk, "Effects of different kinds of fibers on mechanical and tribological properties of brake friction materials," *Tribology Transactions*, Vol. 56, No. 4, (2013), 536-545, doi: 10.1080/10402004.2013.767399.

Persian Abstract

لنت ترمز نقش مهمی در کنترل وسایل نقلیه و ماشین آلات و بعد ایمنی دارد. همیشه نیاز به یک ماده کاربردی جدید با خواص بهبود یافته نسبت به موارد موجود وجود دارد. این مطالعه تحقیقاتی به منظور توسعه یک ماده جدید لنت ترمز متشکل از نانوکامپوزیت پلیمری برای افزایش ویژگیهای فیزیکی، مکانیکی و اصطکاکی در مقایسه با مواد لنت ترمز موجود انجام شد. در این مطالعه، نمونه های نانوکامپوزیت پلیمری توسعه داده شد و خواص فیزیکی آنها یعنی چگالی، جذب آب، روغن و تخلخل مورد ارزیابی قرار گرفت. سختی مکانیکی نمونه های توسعه یافته با سختی سنخ ویکر برآورد شد. ویژگی های اصطکاک نمونه ها و مقادیر سایش با پین یا دستگاه دیسک تعیین می شود. رفتار لغزشی خشک با انجام آزمایشات متعدد با سرعت لغزش در بازه ۲-۱۰ متر بر ثانیه مورد بررسی قرار گرفت و بار از ۲۰ نیوتن به ۱۰۰ نیوتن تغییر کرد تا در مورد تأثیر سرعت، تأثیر فشار تماس اسمی و اثر لغزش بحث شود. فاصله بر روی پارامترهای اصطکاک و دما مورفولوژی نمونه های آماده شده لنت ترمز با میکروسکوپ الکترونی روبشی مشخص شد. میکروگراف های الکترونی روبشی سطوح لنت ترمز نشان داد که بقایای سایش و فلات های مختلف به طور قابل توجهی بر ویژگی های اصطکاک تأثیر می گذارد. نمونه های توسعه یافته به همراه نمونه های تجاری مقاومت بسیار خوبی در برابر جذب آب و روغن نشان می دهند. نتایج بدست آمده برای نمونه های لنت ترمز نانوکامپوزیت پلیمری ارزیابی شده، پتانسیل آنها را برای کاربردهای لنت ترمز نشان می دهد.
